Available online at http://www.journalcra.com

International Journal of Current Research
Vol. 8, Issue, 06, pp.33253-33256, June, 2016

INTERNATIONAL JOURNAL OF CURRENT RESEARCH

ISSN: 0975-833X

RESEARCH ARTICLE

OXYGEN PARTIAL PRESSURE DEPENDENCE PHYSICAL PROPERTIES OF NANOCRYSTALLINE DC MAGNETRON SPUTTERED TIN OXIDE THIN FILMS

[1]Prathyusha, T., [1]Srikanth, T., [1,*]Sivasankar Reddy, A., [2]Kartheek, K., [2]Sreedhara Reddy, P., and [3]Ch. Seshendra Reddy

[1]Department of Physics, Vikrama Simhapuri University Post Graduate Centre, Kavali -524201, Andhra Pradesh, India
[2]Department of Physics, Sri Venkateswara University, Tirupati- 517 502, Andhra Pradesh, India
[3]Department of Materials Science and Engineering, Harbin Institute of Technology, University Town, Shenzhen, 518055, P R China

ARTICLE INFO

Article History:
Received 17th March, 2016
Received in revised form
17th April, 2016
Accepted 21st May, 2016
Published online 30th June, 2016

Key words:

Tin oxide, Thin films, Nanocrystalline, Sputtering, Oxygen partial pressure.

ABSTRACT

Nanocrystalline tin oxide (SnO_2) thin films were deposited on glass substrates by DC reactive magnetron sputtering technique under various oxygen partial pressures. The films composition was nearly stoichiometery at the oxygen partial pressure of $7x10^{-4}$ mbar. XRD pattern reveals that the films are polycrystalline nature and (110) plane was predominant. The size of grains becomes bigger and spherical in shape with increasing of the oxygen partial pressure. The films show high optical transmittance of 93% at the oxygen partial pressure of $7x10^{-4}$mbar. The electrical resistivity of the films was decreases with increasing the oxygen partial pressure.

Citation: Prathyusha, T., Srikanth, T., Sivasankar Reddy, A., Kartheek, K., Sreedhara Reddy, P. and Ch. Seshendra Reddy, 2016. "Oxygen partial pressure dependence physical properties of Nanocrystalline dc magnetron sputtered tin oxide thin films", *International Journal of Current Research*, 8, (06), 33253-33256.

INTRODUCTION

Tin oxide (SnO_2) thin films have wide range of applications such as gas sensors, antireflection coatings, catalysis, displays, transparent electrodes, and solar cells (Ichimura *et al*., 2004; Afify *et al*., 1996; Chaparadza and Rananavare, 2010), due to its wide band gap, high transparency, mechanically harder than ZnO thin films, high chemical and thermal stability (Çetinörgü *et al*., 2007). In the past few years, much attention has been focused on the synthesis and investigation of the novel properties of nanocrystalline SnO_2 for gas sensor applications (Chen *et al*., 2004; Schierbaum *et al*., 1992). The sensitivity of SnO_2 gas sensors increases drastically with decreasing the grain size from 20 to 5 nm (Tricoli *et al*., 2008). Various thin film preparation techniques including reactive thermal evaporation, electron beam evaporation (Rajesh Kumar *et al*., 2012), sputtering (Sivasankar Reddy *et al*., 2012), spray pyrolysis (Boben Thomas and Benoy Skariah, 2015) and spin-coating (EL Sayed *et al*., 2016), have been used to deposit SnO_2 films. Among these techniques, DC reactive magnetron sputtering is one of the best technique due to its high deposition rates, easy control over the composition of the deposited films, reproducibility, and ability to provide uniform coatings over large areas substrates. In this work, the influence of oxygen partial pressure on the structural, compositional, morphological, optical and electrical properties of SnO_2 films prepared by DC reactive magnetron sputtering has been investigated.

***Corresponding author: Sivasankar Reddy, A.**
Department of Physics, Vikrama Simhapuri University Post Graduate Centre, Kavali -524201, Andhra Pradesh, India.

Experimental

SnO_2 thin films were deposited on glass substrate by dc reactive magnetron sputtering from home made circular planar magnetron sputtering system. The sputter chamber was pumped with diffusion pump and rotary pump combination. The pressure in the sputter chamber was measured using digital pirani and penning gauge combination. The magnetron target assembly was mounted at the top of the sputter chamber such that the sputtering could be done by down configuration. Both flow rates of sputter (argon) and reactive gases (oxygen) were controlled individual by Tylan mass flow controllers. The sputtering condition maintained during the growth of SnO_2 films are mentioned in Table 1.

Characterisation

The chemical composition of films determine by electron probe microanalysis (EPMA). The crystallographic structure of the films was analysed with X -ray diffraction (XRD). The surface morphology and microstructure of the films were analysed with atomic force microscope (AFM) and scanning electron microscope (SEM), respectively. The transmittance of the films was monitored using the Hitachi U-3400 UV-Vis-NIR double beam spectrometer in the wavelength range of 300-1000 nm. The resistivity of the films was measured using vander Pauw method.

Table 1. Deposition parameters maintained during the preparation of SnO_2 films by dc reactive magnetron sputtering

Sputtering target	: Sn (99.9%)
Target to substrate distance	: 60 mm
Ultimate pressure	: $2x10^{-6}$ mbar
Oxygen partial pressure	: $3x10^{-4}$ mbar to $9x10^{-4}$ mbar
Sputtering pressure	: $3x10^{-2}$ mbar
Substrate temperature	: 473 K
Sputtering power	: 40 W

RESULTS AND DISCUSSION

Compositional and structural properties

The chemical composition of as deposited films at different oxygen partial pressures was listed in Table 2. The Sn content was high in the films deposited at low oxygen partial pressure and the atomic percentage of Sn/O was 0.58. As increasing the oxygen partial pressure to $7x10^{-4}$ mbar, the Sn content was decreased and films exhibited nearly stiochiometry.

Table 2. The chemical composition of as deposited films at different oxygen partial pressure

Oxygen partial pressure	Atomic percentage		
	Sn	O	Sn/O
$3x10^{-4}$ mbar	36.8	63.2	0.58
$7x10^{-4}$ mbar	34.1	65.9	0.52

Fig.1. shows the X-ray diffraction pattern of SnO_2 films deposited at different oxygen partial pressures. The as deposited films exhibits polycrystalline nature and represent tetragonal structure of SnO_2 films. The films deposited at low oxygen partial pressures ($\geq 5x10^{-4}$ mbar) exhibited predominant (110) plane with low intensity (200) plane. At optimum oxygen partial pressure of $7x10^{-4}$ mbar the crystallinity and polycrystallinity nature of the films increased greatly. Beyond this optimum oxygen partial pressure the crystallinity of the films decreased and (200) plane was vanished. At higher oxygen partial pressures, excess of oxygen atoms are segregation at grain boundaries and deposited atoms would not have enough mobility to growth in stable plane, consequently peak intensity and polycrystallinity of the films were decreased (Mallikarjuna Reddy *et al*., 2011).

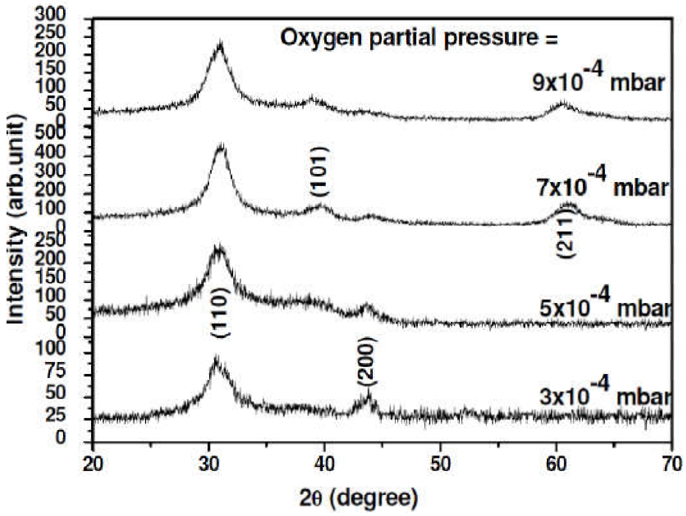

Fig.1. XRD pattern of SnO_2 films at different oxygen partial pressures

The grain size of films was calculated using Scherre's relation (Cullity, 1978),

$$L=k\lambda/\beta\cos\theta \quad ----- (1)$$

where, L is the mean crystalline grain size, k is the correction factor, λ is the wavelength, β is the full width at half maximum in radians. The calculated grain size values of the films at different oxygen partial pressures were listed in Table 3. The increasing of grain size with oxygen partial pressure was due to increases of crystallinity of the films. The lattice parameter *a* and *c* are calculated from (110) and (211) peaks and are listed in Table 3.The lattice parameter *a* increases with the increase of oxygen partial pressure from $3x10^{-4}$ mbar to $7x10^{-4}$ mbar, due to decreasing of oxygen vacancies. The increasing of lattice parameter at higher oxygen partial pressure was due to structural defects in the films.

Table 3. Grain size and lattice parameters values of the films at different oxygen partial pressures

Sample	Oxygen partial pressure (mbar)	Grain size (nm)	Lattice Parameters (Å)	
			a	*c*
SnO_2	$3x10^{-4}$	4.3	4.757	-
	$5x10^{-4}$	4.8	4.749	-
	$7x10^{-4}$	6.1	4.732	3.169
	$9x10^{-4}$	4.6	4.751	3.245
SnO_2 (ICDD)	-	-	4.737	3.186

Surface morphology and Microstructure

The surface morphology of SnO_2 films at different oxygen partial pressures was shown in Fig.2. From the AFM images, the shape and size of the grains were changed with oxygen partial pressure. At low oxygen partial pressure of $3x10^{-4}$ mbar the films exhibited small grains with rms roughness of 1.1 nm and it was increased to 1.6 nm with increasing the oxygen partial pressure to $7x10^{-4}$ mbar. The films show the non-uniform grains with high rms roughness of 2.1 nm at higher oxygen partial pressure of $9x10^{-4}$ mbar.

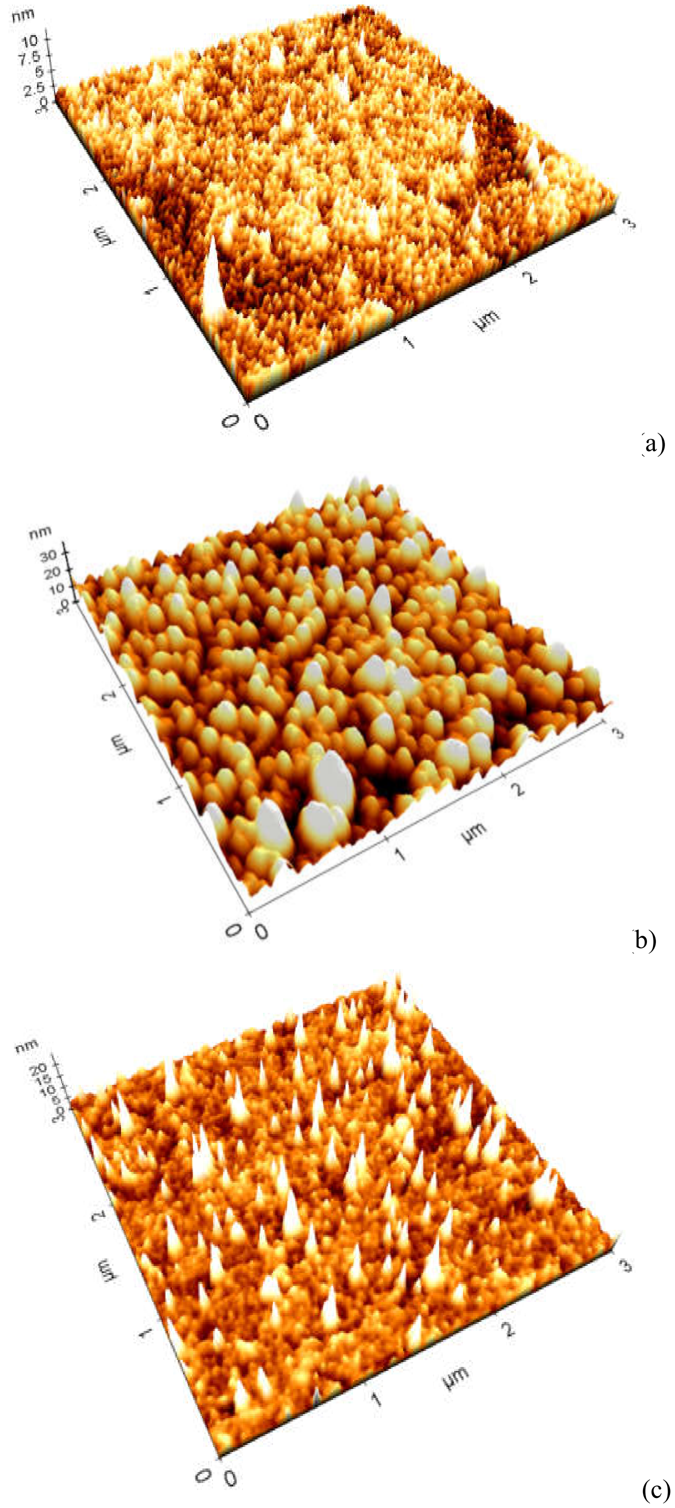

Fig.2. AFM images of SnO_2 films deposited at various oxygen partial pressures: (a) $3x10^{-4}$ mbar, (b) $7x10^{-4}$ mbar and (c) $9x10^{-4}$ mbar

From the SEM images (Fig.3.), at low oxygen partial pressure of $3x10^{-4}$ mbar the films are dense with fine grains. The films deposited at oxygen partial pressure of $7x10^{-4}$ mbar the size of the grains increases and there are no voids, cracks, clusters on the surface of the films. This was due to improvement in crystallinity and decrease in structural defects. At higher oxygen partial pressure of $9x10^{-4}$ mbar the size of grains decreased.

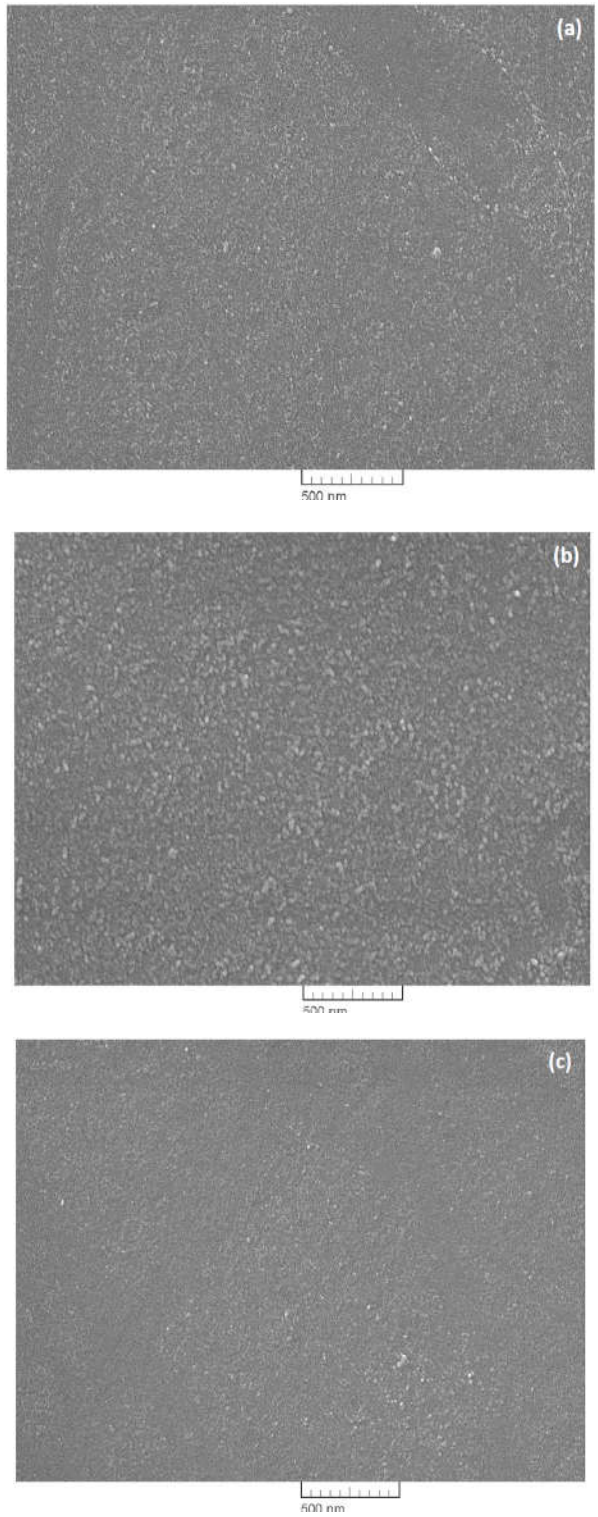

Fig.3. SEM images of SnO_2 films deposited at various oxygen partial pressures: (a) $3x10^{-4}$ mbar, (b) $7x10^{-4}$ mbar and (c) $9x10^{-4}$ mbar

Optical and electrical properties

The optical transmittance spectra of SnO_2 films deposited under various oxygen partial pressures was shown in Fig.4. At low oxygen partial pressure $3x10^{-4}$ mbar the transmittance of the films was 78% which may be due to poor crystallinity and metal rich in the deposited films. As increasing the oxygen partial pressure to $7x10^{-4}$ mbar the transmittance was increased to 93% due to decrease in the density of defect centres. Beyond this oxygen partial pressure the transmittance of the films was decreased to 88%.

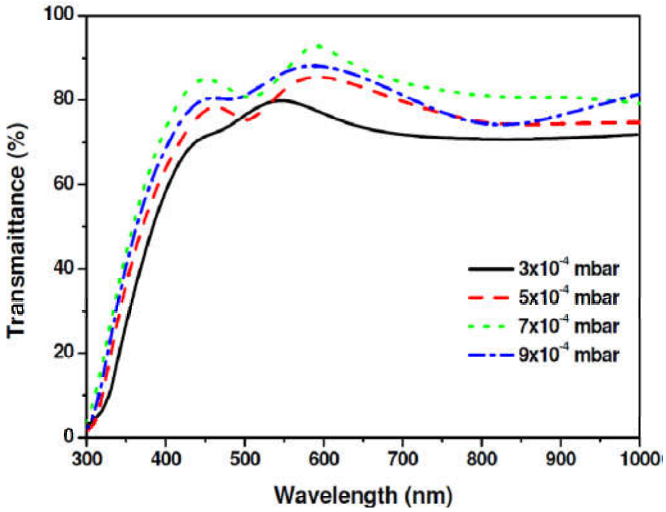

Fig.4. Optical transmittance spectra of SnO_2 films at various oxygen partial pressures

The films show high electrical resistivity of 2.3 Ωcm at low oxygen partial pressure of $3x10^{-4}$ mbar. The electrical resistivity of the films decreases from 0.8 Ωcm to 0.01 Ωcm with increase of oxygen partial pressure from $5x10^{-4}$ mbar to $7x10^{-4}$ mbar. The decrease in electrical resistivity with increasing of oxygen partial pressure was due to increase of the crystallinity and decreases of defects in the films. On further increasing of the oxygen partial pressure to $9x10^{-4}$ mbar the electrical resistivity of the films increased to 0.5 Ωcm.

Conclusion

Nanocrystalline SnO_2 films were deposited on glass substrates under various oxygen partial pressures by using DC reactive magnetron sputtering technique. The stoichiometry and crystalline of the films were increases with increasing the oxygen partial pressure from $3x10^{-4}$ mabr to $7x10^{-4}$. From the microsturcture and surface morphology images, the grain size and smoothness of the films increases with increasing of the oxygen partial pressure. The films exhibited high optical transmittance of 93% with low electrical resistivity of 0.01 Ωcm at oxygen partial pressure of $7x10^{-4}$ mbar.

REFERENCES

Afify, H.H., Terra, F.S., Momtaz, R.S. 1996. Substrate temperature effects on the tin oxide films prepared by spray pyrolysis, *J Mater Science:Mater Electr.,* 7:149-153.

Boben Thomas, and Benoy Skariah, 2015. Spray deposited Mg-doped SnO_2 thin film LPG sensor: XPS and EDX analysis in relation to deposition temperature and doping, *J Alloys & Compounds*, 625:231-240.

Çetinörgü, G.E., Goldsmith, S., Mansur, F. 2007. Optical and structural characteristicsof tin oxide thin films deposited by filtered vacuum arc and spray pyrolysis, *Phys Stat Sol*., (a) 204:3278-3285.

Chaparadza, A. and S.B. Rananavare. 2010. Towards p-type conductivity in SnO_2 nanocrystals through Li doping, *Nanotechnology*, 21:035708.

Chen, Z.W., Lai, J.K.L., Shek, C.H. 2004. Insights into microstructural evolution from nanocrystalline SnO_2 thin films prepared by pulsed laser deposition, *Physical Review B,* 70:165314-165317.

Cullity, B.D. 1978. Elements of X-ray Diffraction, 2nd Ed., Addison Wesley, London.

EL Sayed, A.M., Taha, S., Shaban, M., Said, G. 2016. Tuning the structural, electrical and optical properties of tin oxide thin films via cobalt doping and annealing super lattices and microstructures, 95:1-13.

Ichimura, M., Shibayama, K., Masui, K. 2004. Fabrication of SnO_2 thin films by a photochemical deposition method, *Thin Solid Films,* 466:34-36.

Mallikarjuna Reddy, A., Sivasankar Reddy, A., Kee-Sun Lee, Sreedhara Reddy, P. 2011. Effect of oxygen partial pressure on the structural, optical and electrical properties of sputtered NiO films, *Ceramics International*, 37:2837-2843.

Rajesh Kumar, Atul Khanna, Sastry, V.S. 2012. Interaction of reducing gases with tin oxide films prepared by reactive evaporation techniques, *Vacuum,* 86:1380-1386.

Schierbaum, K.D., Weimar, U., Goepel, W. 1992. Comparison of ceramic, thick-film and thin-film chemical sensors based upon SnO_2, *Sens Actuators*, B 7:709-716.

Sivasankar Reddy, A., Figueiredo, N.M., Cavaleiro, A. 2012. Nanocrystalline SnO_2 and Au:SnO_2 thin films prepared by direct current magnetron reactive sputtering, *Vacuum,* 86:1323-1327.

Tricoli, A., Graf, M., Pratsinis, S.E. 2008. Optimal doping for enhanced SnO_2 sensitivity and thermal stability, *Adv Funct Mater,* 18:1969-1976.

****